

Evidence for the dissipation region in magnetotail reconnection

Seiji Zenitani,¹ Iku Shinohara,² and Tsugunobu Nagai³

Signatures of the dissipation region of collisionless magnetic reconnection are investigated by the Geotail spacecraft for the 15 May 2003 event. The energy dissipation in the rest frame of the electron's bulk flow is considered in an approximate form D_e^* , which is validated by a particle-in-cell simulation. The dissipation measure is directly evaluated from the plasma moments, the electric field, and the magnetic field. Using D_e^* , a compact dissipation region is successfully detected in the vicinity of the possible X-point in Geotail data. The dissipation rate is 45 pWm^{-3} . The length of the dissipation region is estimated to $1-2d_i^{\text{loc}}$ (local ion inertial length). The Lorentz work W , the work rate by Lorentz force to plasmas, is also introduced. It is positive over the reconnection region and it has a peak around the pileup region away from the X-point. These new measures D_e^* and W provide useful information to understand the reconnection structure.

1. Introduction

Magnetic reconnection is one of the most important processes in many plasma systems. It drives various explosive events such as solar flares, substorms in the Earth's magnetosphere, and disruptions in laboratory devices. It is well known that the reconnection process is crucially influenced by the dissipation physics near the reconnection point (X-point). The structure of the dissipation region as well as the accommodated physics is of critical importance for the understanding of the reconnection mechanism. Significant efforts have been made on this subject by theories, numerical simulations, and in situ satellite observations.

In a collisionless kinetic plasma, typically at a distance of the ion inertial length from the X-point, ions decouple from magnetic field lines while electrons remain magnetized. As a consequence, Hall physics plays a role inside the ion-decoupling region. Signatures of Hall physics such as quadruple magnetic field, bipolar normal electric field, and the relevant current loops [Sonnerup, 1979] were confirmed by in situ observations in the terrestrial magnetosphere [Nagai et al., 2001; Øieroset et al., 2001].

Deep inside the ion-decoupling region, there is a thin layer where electrons depart from field lines. A compact dissipation region is located in a close vicinity of the X-point. In addition, recent simulation works suggest that narrow electron jets extend from there, stretching the nonideal layer in the outflow directions [Karimabadi et al., 2007; Shay et al., 2007]. These signatures were recently confirmed by satellite

observations. Nagai et al. [2011] found a compact region with an intense cross-tail current and neighboring electron jets at a super-Alfvénic speed in a magnetotail reconnection event.

Until recently it was not clear how to identify the dissipation region inside the electron nonideal layer. Taking the energy transfer into account, Zenitani et al. [2011a, b] have proposed a general measure of the dissipation region. Using particle-in-cell (PIC) simulations, they distinguished the dissipation region from the outer electron jet, which turned out to be an oblique projection of a non-dissipative current sheet [Hesse et al., 2008; Klimas et al., 2012].

In this Letter, we show in situ observational evidence for the dissipation region in a magnetotail reconnection event.

2. Observation and Analysis

On 15 May 2003, Geotail detected a reconnection event in the premidnight tail. This event was extensively analyzed by Nagai et al. [2011] and so we only repeat important features here. Figure 1 shows key properties from 1053:00 UT to 1058:30 UT on 15 May 2003. All data are presented in the spacecraft (SC) coordinates, because the electric field data are available only in the SC coordinates. During the period of our interest, the SC coordinates are virtually the same as the GSE and GSM coordinates. The rotation angle to the GSE coordinates is less than 2.4° and the angle to the GSM is less than 5° . The satellite position was $(X_{\text{GSM}}, Y_{\text{GSM}}, Z_{\text{GSM}}) = (-27.8, +3.3, +3.5R_E)$ at 1056 UT.

Figure 1a shows magnetic field B_z at 16 Hz, measured from the magnetic field experiment (MGF) [Kokubun et al., 1994]. It suddenly turned from southward ($B_z < 0$) to northward ($B_z > 0$) at 1055:44 UT, as indicated by the red dotted lines. Judging from this and many other signatures [Nagai et al., 2011], Geotail encountered a potential X-point (hereafter X-point) at this time.

Other quantities are shown at 12 s time resolution. Figure 1b shows electric field data, obtained from the electric field detector (EFD) [Tsuruda et al., 1994]. Technically, they were measured every 3 s and then averaged over 12 s. We note that the average electric field during 1057:45 – 1057:58 UT (the arrow in Fig. 1b) is represented by one during 1057:45 – 1057:52 UT, because EFD had violent, high-frequency noises of $\Delta E \sim 50 \text{ mVm}^{-1}$ during 1057:52 – 1057:58 UT. One can see that E_x has a bipolar signature across the X-point. This is a well-known signature of kinetic reconnection (e.g., Hoshino [2005]).

Figures 1c and 1d show the ion and electron bulk velocities. Plasma moments are calculated from distribution functions that are measured by the low-energy particle experiment (LEP) [Mukai et al., 1994]. Due to the low time-resolution of 12 s, these moments contain field-aligned flows along the separatrices from 1055:30 UT to 1057:00 UT. To rule out the field-aligned Hall currents, transverse velocities are presented ($\mathbf{v}_{\perp i}, \mathbf{v}_{\perp e}$). The $v_{\perp ey}$ is distinctly fast near the X-point (Fig. 1d). As seen in Figure 1c, both $v_{\perp ix}$ and $v_{\perp ex}$ change their signs across the X-point. Note that $v_{\perp ex}$ overshoots $v_{\perp ix}$ on both two sides of the X-point. The outward electron velocity is even faster than the typical upstream Alfvén velocity. The upstream magnetic field

¹National Astronomical Observatory of Japan

²Institute of Space and Astronautical Science, Japan Aerospace Exploration Agency

³Tokyo Institute of Technology

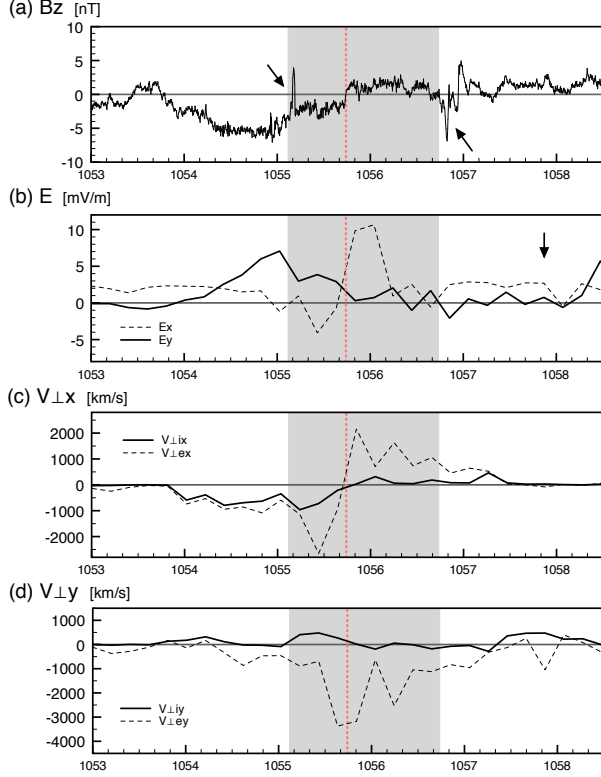


Figure 1. (Color online) Geotail observation from 1053:00 UT to 1058:30 UT on 15 May 2003. (a) Normal magnetic field B_z [nT], (b) electric field E_x , E_y [mV/m], and (c,d) plasma perpendicular velocities [km/s] in the X_{SC} and Y_{SC} directions. A potential X-point (red dotted line) and a characteristic interval from 1055:07 to 1056:44 UT (shadow) are overplotted.

(10 nT) and density (0.01cm^{-3}) give 2200 km/s. Such bi-directional, super-Alfvénic electron jets are consistent with previous simulations [Karimabadi et al., 2007; Shay et al., 2007].

The shadows indicate a characteristic interval from 1055:07 to 1056:44 UT, surrounded by sudden spikes in B_z (Fig. 1a). This interval features super-Alfvénic electron jets (Fig. 1c), an intense duskward electron flow (Fig. 1d), and a low plasma density (not shown). Nagai et al. [2011] referred to this interval as the “ion-electron decoupling time.”

Next we introduce several measures to discuss the reconnection region from Geotail data. We consider the energy transfer in the rest frame of the electron’s bulk flow. This measure, the electron-frame dissipation measure D_e , is formally defined in Eq. (7) in Zenitani et al. [2011a]. In a nonrelativistic neutral plasma, it can be reduced to

$$D_e = \mathbf{j} \cdot \mathbf{E}' = \mathbf{j} \cdot \mathbf{E} - W, \quad (1)$$

where $\mathbf{E}' = \mathbf{E} + \mathbf{v}_e \times \mathbf{B}$ is the nonideal electric field and

$$W = (\mathbf{j} \times \mathbf{B}) \cdot \mathbf{v}_i = (\mathbf{j} \times \mathbf{B}) \cdot \mathbf{v}_e. \quad (2)$$

is the work rate per unit volume by the Lorentz force to the ion fluid or the electron fluid. Since this Lorentz work W (/sec /unit volume) stands for the energy transfer in the ideal MHD, Equation 1 reads the total energy transfer minus the ideal transfer, i.e., the *nonideal* energy transfer

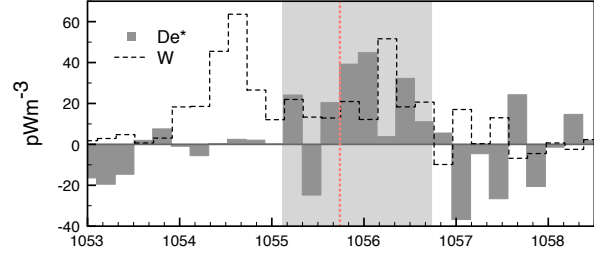


Figure 2. (Color online) The approximate dissipation measure D_e^* (gray histogram) and the work rate by the Lorentz force W (dashed histogram). The X-point (red dotted line) and the interval (shadow) are the same as those in Figure 1.

from fields to plasmas [Birn and Hesse, 2005; Zenitani et al., 2011a]. We further assume $E'_z = 0$ to obtain the following approximate form,

$$D_e^* = j_x E'_x + j_y E'_y. \quad (3)$$

The two measures D_e^* and W are shown in Figure 2. The current density is directly calculated from the plasma moments, $\mathbf{j} = en_i(\mathbf{v}_i - \mathbf{v}_e)$. The dissipation D_e^* (gray histogram) has a peak near the X-point. Its peak rates are 39 and 45 pWm^{-3} during 1055:32 – 1055:44 UT and 1055:44 – 1055:56 UT (two 12 s intervals), respectively. The Lorentz work W (dashed histogram) has a peak during 1054:31 – 1054:43 UT.

3. PIC simulation

We validate our observations with a 2D PIC simulation [Zenitani et al., 2011b]. We employ a Harris-like initial model, $\mathbf{B}(z) = B_0 \tanh(z/L)\hat{\mathbf{x}}$ and $n(z) = n_0[0.2 + \cosh^{-2}(z/L)]$, where B_0 and n_0 are the reference magnetic field and density. The current sheet thickness is set to $L = 0.5d_i$, where d_i is the ion inertial length. Other simulation parameters are $m_i/m_e = 100$, $\omega_{pe}/\Omega_{ce} = 4$, $T_i/T_e = 5$, and 2400×1600 cells with 2.2×10^9 particles. The computational domain is $x, z \in [0, 76.8] \times [-19.2, 19.2]$ in units of d_i with periodic (x) and reflecting (z) boundaries. Velocities are normalized by the typical Alfvén velocity $c_A = B_0/(\mu_0 n_0 m_i)^{1/2}$.

Figure 3 shows snapshots in the well-developed stage. In this case, judging from the sign of D_e , the dissipation region is located around $34.7 < x < 41.5$ and $-0.38 < z < +0.38$. Its thickness is limited by that of an electron current layer. The layer thickness is comparable with the local electron inertial length, $d_e^{\text{loc}} \sim 0.31$. There are also weak dissipative regions at $x = 28$ and $x = 48$, where the magnetic field lines suddenly flip. Surprisingly, both D_e and D_e^* give almost identical pictures, as shown in Figures 3a and 3b. There are minor differences near the vertical dissipative regions but it is hard to recognize them in the figures.

Figure 3c presents plasma outflow velocities along the outflow line ($z = 0$). The electron jet substantially overruns the ion flow [Karimabadi et al., 2007; Shay et al., 2007] until it reaches a shock-like transition region at $x \approx 28$ and $x \approx 48$. The electrons are magnetized further downstream. Note that v_{ix} and v_{ex} are still different in the downstream, because the ions remain unmagnetized.

Figures 3d shows the dissipation measure D_e and the Lorentz work W . The D_e measure is almost identical to D_e^* along the outflow line, where $j_z E'_z \approx 0$. Outside the

central dissipation region, D_e exhibits a weak undershoot in the downstream, indicating energy transfer from plasmas to the electromagnetic fields in the comoving frame of plasmas. This is a signature of the fast electron jet region [Zenitani et al., 2011b]. The Lorentz work W is usually positive over the reconnection region, because the Lorentz force continuously drives plasmas in the outflow directions. Further downstream, it has a local peak at $x \approx 16.5$ (outside the domain in Fig. 3), where the reconnected flux (B_z) hits the initial current sheet.

4. Discussion

Let us examine the validity of the approximate measure (Eq. 3). Since EFD does not measure E_z along the spin axis, we have to reconstruct E_z in Equation 1. We consider the following three ways. (1) A popular way is to assume $\mathbf{E} \cdot \mathbf{B} = 0$. However, since there are strong parallel electric field near the dissipation region, $\mathbf{E}_{\parallel} \neq 0$ [Pritchett, 2001; Wygant et al., 2005], and since B_z is usually weak, this does not work. (2) The second is to assume $E_z = 0$. This gives a different picture that emphasizes separatrices. Physically, this assumption drops the energy transfer $j_z E_z$ but leave the ideal part $j_z(\mathbf{v}_e \times \mathbf{B})_z$ in Equation 1. In other words, the ideal part contaminates the nonideal dissipation measure D_e . Thus we should not assume $E_z = 0$. (3) The third is to set $E'_z = 0$. This is our choice. Despite strong Hall electric field E_z near the dissipation region [Shay et al., 1998; Wygant et al., 2005], the $E'_z \approx 0$ condition is fairly satisfied outside the electron current layer, and so $j_z E'_z$ is a minor contributor to D_e along the inflow line (see Fig. 5a in Zenitani et al. [2011b]). The ideal condition is also violated $E'_z \neq 0$ along the separatrices but this does not involve significant energy transfer. In general, $j_z E'_z$ is negligible due to weak j_z . Thus D_e^* approximates D_e quite well. Note that this choice is specific to a magnetotail configuration without a guide field. In other configurations $j_z E'_z$ could be important and Equation 3 may not be useful.

In Figure 2, the D_e^* measure has a peak near the X-point during 1055:44 – 1056:08 UT. This is evident for the dissipation region. Let us evaluate the dissipation rate. The reconnection electric field E_y is fairly uniform over the reconnection region, except for the magnetic pile-up region near the outflow jet front. From PIC simulations, we empirically know that the reconnection rate remains constant, $E_y \approx 0.1 c_{A,up} B_{up}$. Here, B_{up} and $c_{A,up}$ are the magnetic field and the Alfvén velocity in an upstream region, typically a few d_i upstream from the X-point. It is empirically known that the half width of the electron current layer is approximated by the local electron inertial length d_e^{loc} up to the case of a realistic mass ratio [Pritchett, 2010]. The current density inside the dissipation region is $j \sim B_d/(\mu_0 d_e^{loc})$, where B_d is the magnetic field at the upstream edge of the dissipation region. After the initial current sheet plasma moves out, the plasma density is roughly uniform over the reconnection region. Assuming a uniform density, one can estimate typical dissipation at the X-point,

$$\begin{aligned} D_e^* &\approx \left(\frac{B_d}{\mu_0 d_e^{loc}} \right) (0.1 c_{A,up} B_{up}) \\ &= 326 \left(\frac{B_d}{B_{up}} \right) \left(\frac{B_{up}}{10 \text{ nT}} \right)^3 \text{ pWm}^{-3}. \end{aligned} \quad (4)$$

From simulations, we know that the upstream magnetic field is typically a half of the asymptotic lobe field: $B_{up} \sim \frac{1}{2} B_0$. In this event, the lobe field is estimated to $B_0 = 20$ nT, while B_x occasionally hits 10 nT near the separatrices. Thus, it would be reasonable to assume $B_{up} = 10$ nT. Meanwhile, it is very difficult to estimate B_d , because the electron-scale

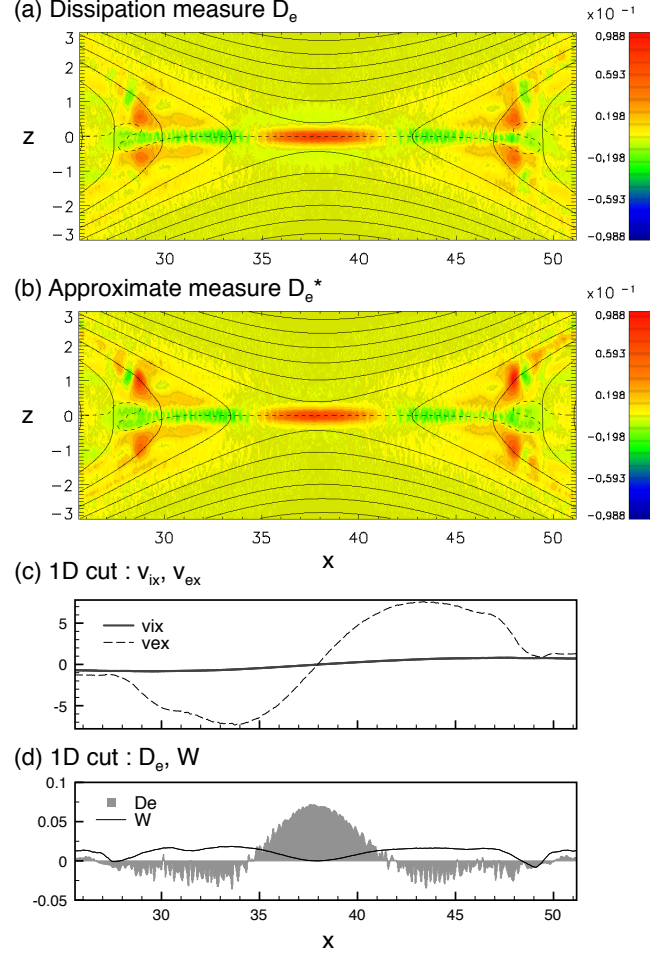


Figure 3. (Color online) (a) The dissipation measure D_e (Eq. 1) in unit of $J_0 c_A B_0$ with magnetic field lines superposed, (b) the approximate dissipation measure D_e^* (Eq. 3) in the same unit, (c) v_{ix}, v_{ex} at $z = 0$, and (d) the dissipation measure D_e and the Lorentz work W at $z = 0$.

dissipation region is embedded in a thick reconnection layer of the order of the ion meandering width. From simulation we obtain $(B_d/B_{up}) \approx 0.5$. However, this ratio could be smaller in a real system, because the electron skin depth with $m_i/m_e = 1836$ is 4.3 times smaller than one with $m_i/m_e = 100$. Using $B_{up} = 10$ nT and $(B_d/B_{up}) < 0.5$, we obtain $D_e^* < 163 \text{ pWm}^{-3}$. In addition, our data are averaged over a time interval of 12 s. Geotail resolves the spatial structure rather coarsely. Using spatially averaged quantities, their product D_e^* could be underestimated by a factor of two or three. Considering this, the observed rates, 39 and 45 pWm^{-3} (1055:44 – 1056:08 UT), are reasonable.

It is difficult to evaluate unambiguously the size of the dissipation region in our single-satellite observation. Shay et al. [2007] predicted that the half length of the $E'_y > 0$ region is $\sim 0.6 d_i$. In many $m_i/m_e = 25$ runs [A. Klimas, private communication] and in our $m_i/m_e = 100$ run, the dissipation region is twice longer than the $E'_y > 0$ region. Thus the full length of the dissipation region will be $2.4 d_i$. On the other hand, Zenitani et al. [2011b] reported that the aspect ratio of the dissipation region is ~ 0.1 . Given that the half width of the dissipation region is $\sim d_e^{loc}$, the full length will be $\sim 20 d_e^{loc} \sim 0.47 d_i^{loc}$. In these cases, the full

extent of the dissipation region will be

$$2.4d_i \sim 1726 \left(\frac{n_i}{0.1\text{cm}^{-3}} \right)^{-1/2} \text{ km}, \quad (5)$$

$$0.47d_i^{\text{loc}} \sim 1061 \left(\frac{n_i^{\text{loc}}}{0.01\text{cm}^{-3}} \right)^{-1/2} \text{ km}. \quad (6)$$

Examining several clues such as the upstream distribution functions, Nagai et al. [2011] estimated that the entire structure retreats at ~ 100 km/s. The above two estimates are comparable with the spatial scale of one or two sampling intervals (12–24 s), 1200–2400 km. Geotail detected the dissipation region by two or three sampling intervals (Fig. 2), 2400–3600 km or $3\text{--}5d_i$ or $1\text{--}2d_i^{\text{loc}}$. The length of the dissipation region is on the same order.

The characteristic interval from 1055:07 to 1056:44 UT (the shadow regions in Figs. 1 and 2) would correspond to the full extent of the outer electron jet region in the PIC simulation ($28 < x < 48$ in Fig. 3). One can recognize the magnetic field fluctuations in Figure 1a (indicated by arrows). It is likely that the fluctuations originate from the electron jet front region at $x \approx 28$ and $x \approx 48$ (Fig. 3), where the fast electron jet hits the outer plasma outflow. In observation, D_e^* is negative before the central dissipation region arrives (Fig. 2). This is consistent with the weak undershoot of D_e in the electron jet region in the PIC simulation (Fig. 3). We do not recognize a similar undershoot on the other side (1055:44 – 1056:44 UT). This is because the Geotail was near the separatrix, outside the central electron jet region [Nagai et al., 2011]. It is not surprising that $v_{\perp i}$ still differs from $v_{\perp e}$ outside the interval (Figs. 1c and 1d). Electrons are magnetized there, but ions remain unmagnetized downstream of the electron jet fronts. Reconnection outflow recovers the ideal MHD approximation when ions are magnetized further downstream, but the transition to the MHD region could be ambiguous.

As seen in Figure 2, the Lorentz work W is usually positive over the reconnection region. This signature is consistent with the PIC simulation (Section 3). One can recognize a peak during 1054–1055 UT. We find that B_z is compressed (Fig. 1a) in this interval and that the plasma density decreased after the W -region arrived (see Fig. 1j in Nagai et al. [2011]). This W -region appears to be a magnetic pile-up region behind a tangential discontinuity, where the compressed B_z pushes the dense plasma sheet outward. We do not recognize similar W -region on the other side of 1057–1058 UT, because the satellite was not in the central neutral plane. In fact, we find similar W -regions associated with the pile-up regions in other reconnection events. The W measure in reconnection deserves further investigation by theories, simulations, and observations.

To our knowledge, this is the first identification of the dissipation region in magnetotail reconnection. Earlier observations focused on large-scale signatures of the reconnection site, such as the flow reversal or Hall fields. In the 15 May 2003 event, Geotail fortunately resolved a small-scale signatures of bi-directional electron jets [Nagai et al., 2011] and then the present work finally detected a compact dissipation region between the jets. Although our resolution is quite limited, this is the best possible measurement with the present instruments. In addition, this work is a step forward for reconnection theories. The dissipation measure theory [Zenitani et al., 2011a] was only tested by 2D PIC simulations with artificial mass ratio. Here we showed that the theory works in the complex real world. The theory appears to be practically useful.

5. Conclusion

We analyzed Geotail reconnection event on 15 May 2003. We applied the electron-frame dissipation measure $D_e(D_e^*)$ to the reconnection structure. Using D_e^* , for the first time,

we identified the dissipation region around the possible X-point in nature. The dissipation rate (45pWm^{-3}) and the length of the dissipation region ($1\text{--}2d_i^{\text{loc}}$) are reasonable. We introduced the Lorentz work W as well. The two measures are useful for better understanding of the reconnection structure.

Our approach will be applicable to next-generation in situ observations. NASA’s upcoming Magnetospheric Multiscale (MMS) mission features high temporal resolution, multi-satellite observation, and measurement of all three components of the electric field. We will be able to see clearer pictures of the dissipation region.

Acknowledgments. S.Z. acknowledges S. Imada, M. Hoshino, Y. Miyashita, M. N. Nishino, and M. H. Saito for useful advices.

References

- Birn, J., and M. Hesse (2005), Energy release and conversion by reconnection in the magnetotail, *Ann. Geophys.*, **23**, 3365–3373, doi:10.5194/angeo-23-3365-2005.
- Hesse, M., S. Zenitani, and A. Klimas (2008), The structure of the electron outflow jet in collisionless magnetic reconnection, *Phys. Plasmas*, **15**, 112102, doi: 10.1063/1.3006341.
- Hoshino, M. (2005), Electron surfing acceleration in magnetic reconnection, *J. Geophys. Res.*, **110**, A10215, doi:10.1029/2005JA011229.
- Karimabadi, H., W. Daughton, and J. Scudder (2007), Multi-scale structure of the electron diffusion region, *Geophys. Res. Lett.*, **34**, L13104, doi:10.1029/2007GL030306.
- Klimas, A., M. Hesse, and S. Zenitani (2012), Particle-in-cell simulation of collisionless undriven reconnection with open boundaries, *Phys. Plasmas*, **19**, 042901, doi:10.1063/1.3699032.
- Kokubun, S., T. Yamamoto, M. H. Acuña, K. Hayashi, K. Shiokawa, and H. Kawano (1994), The GEOTAIL magnetic field experiment, *J. Geomagn. Geoelectr.*, **46**, 7–21.
- Mukai, T., S. Machida, Y. Saito, M. Hirahara, T. Terasawa, N. Kaya, T. Obara, M. Ejiri, and A. Nishida (1994), The low energy particle (LEP) experiment onboard the GEOTAIL satellite, *J. Geomagn. Geoelectr.*, **46**, 669–692.
- Nagai, T., I. Shinohara, M. Fujimoto, M. Hoshino, Y. Saito, S. Machida, and T. Mukai (2001), Geotail observations of the Hall current system: Evidence of magnetic reconnection in the magnetotail, *J. Geophys. Res.*, **106**, 25,929–25,949, doi:10.1029/2001JA900038.
- Nagai, T., I. Shinohara, M. Fujimoto, A. Matsuoka, Y. Saito, and T. Mukai (2011), Construction of magnetic reconnection in the near-Earth magnetotail with Geotail, *J. Geophys. Res.*, **116**, A04222, doi:10.1029/2010JA016283.
- Øieroset, M., T. D. Phan, M. Fujimoto, R. P. Lin, and R. P. Lepping (2001), In situ detection of collisionless reconnection in the Earth’s magnetotail, *Nature*, **412**, 414–417, doi:10.1038/35086520.
- Pritchett, P. L. (2001), Collisionless magnetic reconnection in a three-dimensional open system, *J. Geophys. Res.*, **106**, 25961, doi:10.1029/2001JA000016.
- Pritchett, P. L. (2010), Onset of magnetic reconnection in the presence of a normal magnetic field: Realistic ion to electron mass ratio, *J. Geophys. Res.*, **115**, A10208, doi:10.1029/2010JA015371.
- Shay, M. A., J. F. Drake, R. E. Denton, and D. Biskamp (1998), Structure of the dissipation region during collisionless magnetic reconnection, *J. Geophys. Res.*, **103**, 9165, doi:10.1029/97JA03528.
- Shay, M. A., J. F. Drake, and M. Swisdak (2007), Two-Scale Structure of the Electron Dissipation Region during Collisionless Magnetic Reconnection, *Phys. Rev. Lett.*, **99**, 155002, doi:10.1103/PhysRevLett.99.155002.

- Sonnerup, B. U. Ö. (1979), Magnetic field reconnection, in Solar System Plasma Physics, vol. 3, Solar System Plasma Processes, edited by L. T. Lanzerotti, C. F. Kennel, and E. N. Parker, pp. 45–108, North-Holland, New York.
- Tsuruda, K., H. Hayakawa, M. Nakamura, T. Okada, A. Matsuoka, F. S. Mozer, and R. Schmidt (1974), Electric field measurements on the Geotail satellite, *J. Geomagn. Geoelectr.*, *46*, 693–711.
- Wygant, J. R., et al. (2005), Cluster observations of an intense normal component of the electric field at a thin reconnecting current sheet in the tail and its role in the shock-like acceleration of the ion fluid into the separatrix region, *J. Geophys. Res.*, *110*, A09206, doi:10.1029/2004JA010708.
- Zenitani, S., M. Hesse, A. Klimas, and M. Kuznetsova (2011a), New Measure of the Dissipation Region in Collisionless Magnetic Reconnection, *Phys. Rev. Lett.*, *106*, 195003, doi:10.1103/PhysRevLett.106.195003.
- Zenitani, S., M. Hesse, A. Klimas, C. Black, and M. Kuznetsova (2011b), The inner structure of collisionless magnetic reconnection: The electron-frame dissipation measure and Hall fields, *Phys. Plasmas*, *18*, 122108, doi:10.1063/1.3662430.
-
- Seiji Zenitani, National Astronomical Observatory of Japan, 2-21-1 Osawa, Mitaka, Tokyo 181-8588, Japan. (seiji.zenitani@nao.ac.jp)
- Iku Shinohara, Institute of Space and Astronautical Science, Japan Aerospace Exploration Agency, 3-1-1 Yoshinodai, Chuo, Sagami-hara, Kanagawa 252-5210, Japan (iku@stp.isas.jaxa.jp)
- Tsugunobu Nagai, Tokyo Institute of Technology, Tokyo 152-8551, Japan (nagai@geo.titech.ac.jp)